Chemical Engineering Journal 394 (2020) 124960

Contents lists available at ScienceDirect

Chemical Engineering Journal

journal homepage: www.elsevier.com/locate/cej

A highly sensitive and wearable pressure sensor based on conductive polyacrylonitrile nanofibrous membrane via electroless silver plating

Yixiang Chen, Zehong Wang, Rui Xu, Wei Wang, Dan Yu*

College of Chemistry, Chemical Engineering and Biotechnology, Donghua University, Shanghai 201620, China

HIGHLIGHTS

- Electroless plating Pd-activated nanofibrous membranes.
- The electrodes with a nylon network are assembled into a sensitive pressure sensor.
- The capacitive pressure sensor is suitable for practical human motions' detection.

GRAPHICAL ABSTRACT

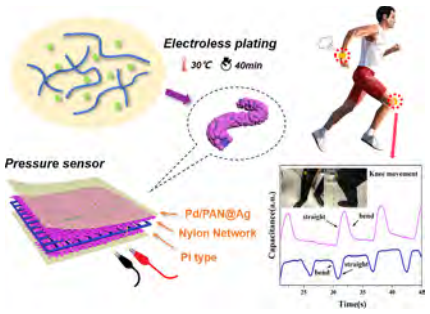

ARTICLE INFO

Keywords:
Capacitance pressure sensor
Nanofibrous membranes
Electroless plating
High sensitivity
Low hysteresis

ABSTRACT

The flexible and wearable capacitive pressure sensors are widely used in healthcare monitoring, robotics manufacture and military equipment. These types of highly sensitive pressure sensors can be realized by designing micro-structure electrodes or dielectric layers on a wearable smart device. Herein, we prepare a flexible and conductive electrode through electrospinning of palladium ions (Pd^{2+})/polyacrylonitrile (PAN) solution and followed by electroless plating of the hybrid nanofibrous membranes. The FESEM images showed that the obtained conductive nanofibrous membrane was covered by a coral-like silver layer with porosity benefiting for excellent electrical conductivity. Based on the superior performance, it is used as the electrodes and jointly assembled into a full microporous structure sensor with the high-mesh nylon netting. Benefitting from the dramatically alterable contact area of the electrode and the good dielectricity of nylon netting, the as-prepared sensor exhibits a high sensitivity of 1.49 kPa^{-1}, a fast response time of 48 ms, low hysteresis of 7.55% and stable durability over 1000 cycles. Besides, practical human motions' detection is carried out by this wearable pressure sensor. The simulation of the finite elemental analysis is used to explain the mechanism of the sensor. This fabrication method is facile, low-cost, and less metal pollution, which may provide an insight to design microstructures for improving the performance, and imply an accessible prospect in the industrialization of sensors.

1. Introduction

Flexible, lightweight and wearable pressure sensors play an important role in the future development of artificial intelligence, especially in health care applications [1], soft robot [2], and military field [3]. According to different sensing mechanisms, piezoresistive [4], capacitive [5], piezoelectric [6], and optical sensing are designed to be applied in daily use [7]. The strain sensor can alter the relevant value responding to external mechanical deformations, and then converts it into a distinct electrical signal. Among these, capacitive pressure

* Corresponding author at: 2999 North Renmin Road, Songjiang District, Shanghai 201620, China.
E-mail address: yudan@dhu.edu.cn (D. Yu).

https://doi.org/10.1016/j.cej.2020.124960
Received 19 December 2019; Received in revised form 27 February 2020; Accepted 2 April 2020
Available online 06 April 2020
1385-8947/

sensors stand out prominent properties including high sensitivity, fast response speed, low fabrication cost [8], low power consumption, and good temperature stability, which widely wins public attention [9] in artificial intelligence and electric skins. But there are some defects of poor measurement accuracy and parasitic capacitance, the pursuit of higher sensitivity is a key issue. Moreover, high equipment requirements and complex processing technology also limit their usability and reproducibility [10].

Generally, high sensitivity can be achieved by designing the microstructure of touching interface [11], suitable assembling method and materials between conductive electrodes and dielectric layers [12]. Thus far, the main focus is on the employment of microporous material or surface modification of dielectric [13], for instance, Zhiguang Qiu et al. reported a tactile sensor with a templated and microstructural dielectric layer using the biomimetic leaf in ionic skins. The sensor had a low-pressure detection limit, a broad-range pressure, a high sensitivity and applied in human-machine interaction [14]. Wen Chen et al. designed a platinum sputtered PDMS electrode with a layered pyramid microstructure, and this sensor with a high specific surface had low hysteresis (~4.42%), high sensitivity, and potential for electronic skins [15]. Therefore, we can see assembling a capacitive pressure sensor with high sensitivity and quick response time needs specific surface microstructure of electrodes or dielectric layers.

Many fabrication methods of conductive materials were reported to fabricate a flexible electrode through the synthesis of carbon materials [16], in-situ polymerization [17] and metallic coating [18,19]. Among these, electroless plating is an efficient and simple metallization depositing method on flexible substrates, which endows conductivity without damaging substrates' natural properties. Herein, we plan to choose the nanofibrous membrane as a substrate because of its lightweight, high specific surface area and porosity. To electroless plating a nanofibrous membrane is a meaningful attempt based on our previous experience on electroless plating and electrospinning [20,21]. We believe the combination of them can bring an ideal electrode suiting for pressure sensors. Furthermore, we have done some improvement after investigated previous research. For example, Lingdi Shen et al. once used polydopamine (DOP) to coat the polyacrylonitrile membranes, then reduce the Ag^+ in the membranes to obtain a uniform and continuous metal layer [22]. But the coating of DOP has an adverse influence on the membrane's physical properties of porosity and breathability. Lifeng Zhang et al. firstly pretreat nanofibrous members through $NH_3{\cdot}H_2O$ agents, and activated by typical dipping in $SnCl_2$ and $PdCl_2$, finally electroless plating to acquire nanofibers surface-decorated with silver nanoparticles [23]. To our knowledge, the use of $SnCl_2$ will definitely cause environmental pollution and the whole process is tedious and complicated.

Therefore, we propose prepared firstly an active nanofibrous membrane through electrospinning of the Pd^{2+}/PAN mixed solution, in which the role of Pd^{2+} is used to activate the following electroless plating. The homogeneously embedded $PdCl_2$ in the membrane not only increase the utilization efficiency of precious metal, but also greatly improve the growth of silver and thus enabling the high conductivity of the resultant membrane. Then, by changing the concentration of silver nitrate, we can regulate the surface deposition and the conductivity of electrodes. Then nylon is employed due to its lightweight, soft and dielectric performance in the case of a high mesh number which facilitates sensitivity and response speed according to literature [24,25]. A sandwich structure capacitive pressure sensor consisting of a 400 mesh nylon netting, two stretchable PAN electrodes and sealed by polyimide (PI) tape at each end is fabricated as shown in Fig. 1. Scanning electron microscope (SEM), field emission scanning electron microscopy (FESEM), energy dispersive spectrometer (EDS), X-ray diffraction (XRD), thermogravimetric analyses (TG), and X-ray photoelectron (XPS) methods were used to characterize the performance of materials. Besides, the application measurements of sensitivity, response time, durability, finger motions, joint movements were investigated. The simulation of ANSYS was used to explain the principle analysis of the high-sensitivity pressure sensor. This microporous self-made sensor had demonstrated many outstanding properties as we expected.

2. Experimental

2.1. Materials

Polyacrylonitrile (PAN, Mw = 150,000) was obtained from Huachuang Group (Anhui, China). The N, N-dimethylformamide (DMF) and ammonia water ($NH_3{\cdot}H_2O$) were supplied by Shanghai Ling Feng chemical reagents Co. Ltd. (Jiangsu, China), anhydrous alcohol was offered from Shanghai and Chemical Co. Ltd. Palladium chloride, silver nitrate ($AgNO_3$, 99.8%), ethylenediamine, glucose, and polyethylene glycol 1540 were procured directly from Sinopharm Chemical Reagent Co. Ltd. (Shanghai, China). The above drugs were analytic reagents without further purification.

2.2. Preparation of PAN nanofiber containing palladium chloride

First, palladium chloride was dissolved in DMF for 8 h at room temperature to acquire a solution with concentration of 1.7 ppm. Then, added PAN powders to the above solution by stirring overnight and stewed to remove the air bubbles before obtaining an 8.0 wt% uniform solution. Finally, the stock solution for electrospinning was fed into a disposable syringe at room temperature with humidity of 50%, an applied voltage was set as 18 kV and the spinneret diameter was 0.67 mm, the propulsion speed was set at 0.55 ml/h, the typical collection distance was 12 cm. After 12-hour spinning time, the PAN nanofibrous membranes containing palladium chloride were formed.

2.3. Formation preparation of the silver-coated membranes by electroless plating

The silver plating solution was made by combining two parts at the volume ratios of 1:1. The reduction solution was: 1.5 g of glucose and 0.06 g of polyethylene glycol were dissolved in 47 ml of deionized water and 3 ml ethanol to form a homogenous solution. The composition of the silver plating solution was: the $AgNO_3$ solution (4 g/L, 8 g/L, 12 g/L) was prepared with different quality $AgNO_3$ and 49 ml deionized water respectively, then the ammonium hydroxide was added dropwise into $AgNO_3$ solution until the precipitate disappeared and solution became clarification again, after that, 1 ml of ethylenediamine was mixed. The samples were immersed in the above reducing solution for 5 s, followed by the plating solution was poured into quickly, electroless plating was afterward maintained in an ultrasonic wave generator for 40 min at room temperature, then washed with deionized water and dried to obtain a silver-plated PAN nanofibrous membrane.

2.4. Preparation of nylon netting

Customized nylon netting with a number of holes of 400 meshes was cut a thin membrane with a size of 30 × 30 mm^2 as a dielectric layer.

2.5. Fabrication of capacitive sensor array

The sandwich-like structure sensor was assembled by two conductive layers as the sensitive electrode and a dielectric layer. Prepared conductive silver-plated PAN nanofibrous membranes were used for the upper and lower electrode plate respectively. The intermediate dielectric membrane was made of customized soft 400 mesh nylon netting that was provided expediently. For the convenience of different testing, two pressure sensors with the contact area of 22 × 23 mm^2 and 15 × 15 mm^2 were prepared. Polyimide tape was as the elastomeric substrate to adhere tightly so as to eliminate the interference of air and simultaneously encapsulated to form a capacitive type sensor model.

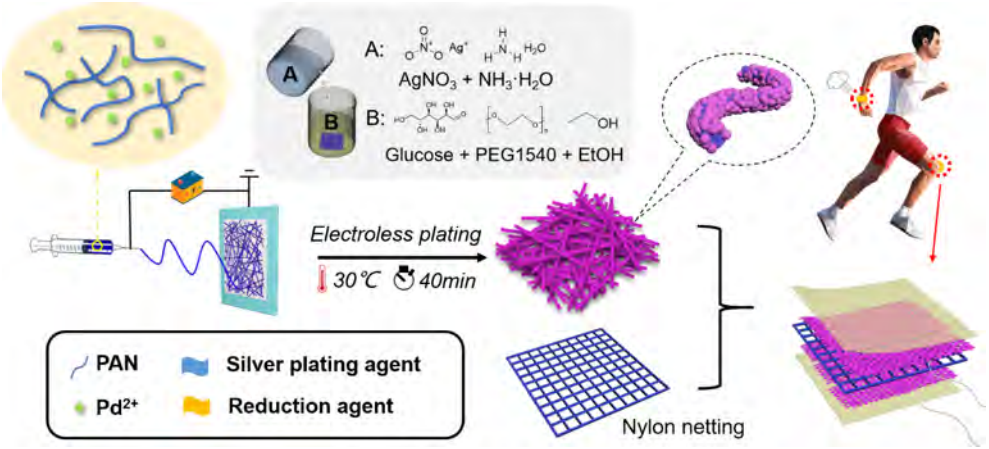

Fig. 1. The schematic illustration of the silver-plated nanofibrous membrane electrode and the assembled sandwich-structure sensor.

2.6. Characterization and measurement

The surface morphology of the nylon netting with 400 mesh was carried out using SEM (TM-1000, Hitachi). The morphology of nanofibers was carried out by FESEM (S-4800), and element composition of membranes with silver was evaluated using EDS (Quanta250). TG (Netzsch 209F1, Germany) was used to characterize the thermal stability of samples from 20 ℃ to 900 ℃ at a heating rate of 20 ℃ min^{-1}. XRD patterns of membranes were performed with D/Max2550 to determine the crystal structure. In order to identify the elements and the chemical bond, XPS was examined. The capacitance of pressure sensors was determined using the digital Multimeter (Keithley DMM6500 6½). Ansys Workbench software was used to simulate and analyze the shape and structural response to external stimulus.

3. Results and discussion

3.1. Preparation of conductive Pd/PAN@Ag membranes

Fig. 1 shows the schematic illustration of the silver-plated nanofibrous membrane electrode and the assembled sandwich-structure sensor. A piece of nylon netting that equipped with two self-made conductive nanofibrous membranes as upper and lower electrodes, and the insertion method of lead wire is to press the conductive copper wire on the surface of the electrode, and the copper wire is evenly coated with a layer of silver paste through a syringe. Then, the nanofibrous membrane is placed in an oven and baked at 90 ℃ for 1 h to cure the silver paste, and the copper wire is firmly fixed on the electrode. The middle layer is selected from a nylon mesh layer as a dielectric layer, and the effective overlap area is 22 × 23 mm^2. The three layers are combined and sealed by a PI tape as a capacitive pressure sensor.

3.2. Characterization and conducting performance of Pd/PAN@Ag membranes

Fig. 2(a) is the measured PAN@Ag membranes at the different metal deposition by controlling the concentration addition of $AgNO_3$. As predicted, with the concentration of $AgNO_3$ being increased to form more conductive connected loop, which leads to decrease sheet resistance and strengthen coating fastness. As-prepared electrode can lighten a bulb with bright light (Fig. 2b). Obviously, when mixing with $PdCl_2$ under the condition of 4 g/L $AgNO_3$, the sheet resistance reduces over four magnitudes compared with the samples without the Pd-activated process. Therefore, 8 g/L $AgNO_3$ with deposition density of 11 mg/cm^2 and the sheet resistance of 0.825 Ω/sq is an appropriate concentration to take into account conductivity and economy synthetically.

Fig. 2(c-f) depict the FESEM images of samples. The images of PAN and Pd/PAN nanofibrous membranes are shown in Fig. 2(c-d), respectively. It seems that the surface of pristine PAN nanofibers is both thin and smooth with average diameters of about 247 nm compared with the images of nanofibers with a small amount of Pd at the average size of 233 nm, the latter decreases in diameter. To obtain high conductivity, silver is deposited by electroless plating onto membranes in Fig. 2(e), and the average diameter of nanofibers is 291 nm. However, the surface of the non-activated nanofibrous membrane is less attached by the silver, and there is a desultory connection among the nano-silver, which also confirms the reason for the high sheet resistance. The image of Fig. 2(f) indicates that Pd-activated conductive PAN nanofibrous membranes can be observed that the nano-silver particles are spherical or partially nano-silver adhere to each other. Finally, the surface of the nanofibers is uniformly coated with a dense continuous coral-like silver layer which produces excellent electrical conductivity, and the average diameters of the nanofibers increase to 481 nm. Hence, the FESEM images indicate that the mixture of palladium to the spinning solution firstly can efficiently initiate the following electroless plating.

Subsequently, the surface elemental composition and element distribution of Pd/PAN@Ag were analyzed by EDS in Fig. 2(g). PAN nanofibrous membranes contain 7.16% C atom and 1.85% of N atom, which slightly exceeded the carbon and oxygen element compared to PAN molecular formula. This may come from the excess glucose solution during the reaction and moisture. Meanwhile, the images of these elements are clearly seen that the Pd ionic was successfully introduced in the nanofibrous membranes. And it also can be seen that Pd (purple dots) and Ag (red dots) species are dispersed evenly on the PAN nanofibrous membranes, correspond to 0.31% and 89.89%. In this work, Pd/PAN nanofibrous membranes obtain uniform Pd(2+) activation sites after electrospinning, and the addition of glucose can reduce Pd (2+) to Pd(0) in the following electroless plating [26], meanwhile, the existence of Pd(0) will act as the activation center to initiate silver plating successfully.

The substance formed on the surface of the nanofibrous membrane can use XPS to analyze composition. The obtained spectra is shown in Fig. 3(a-e), the single peak of N1s in 399 eV presents the C≡N [27], and in the C1s region, two adjacent peaks position are located at 284.19 and 285.77 eV respectively [21], which are associated with C–C and C≡N. These correlative characteristic peaks demonstrate the existence of PAN. In Fig. 3(d), the binding energies with a difference of 6 eV between 373.34 and 367.34 eV, which are related to Ag 3d5/2 and Ag 3d3/2, proves the production of metallic silver(0) [28,29]. In Fig. 3(e), the peaks locate at 196.4 eV likely corresponds to the existence of Cl^- bonded with silver [30]. And the binding energy of 198 eV presents the typical peak of $PdCl_2$ [31]. The introduction of chloride ions can be speculated that $PdCl_2$ is successfully mixed in the nanofibrous

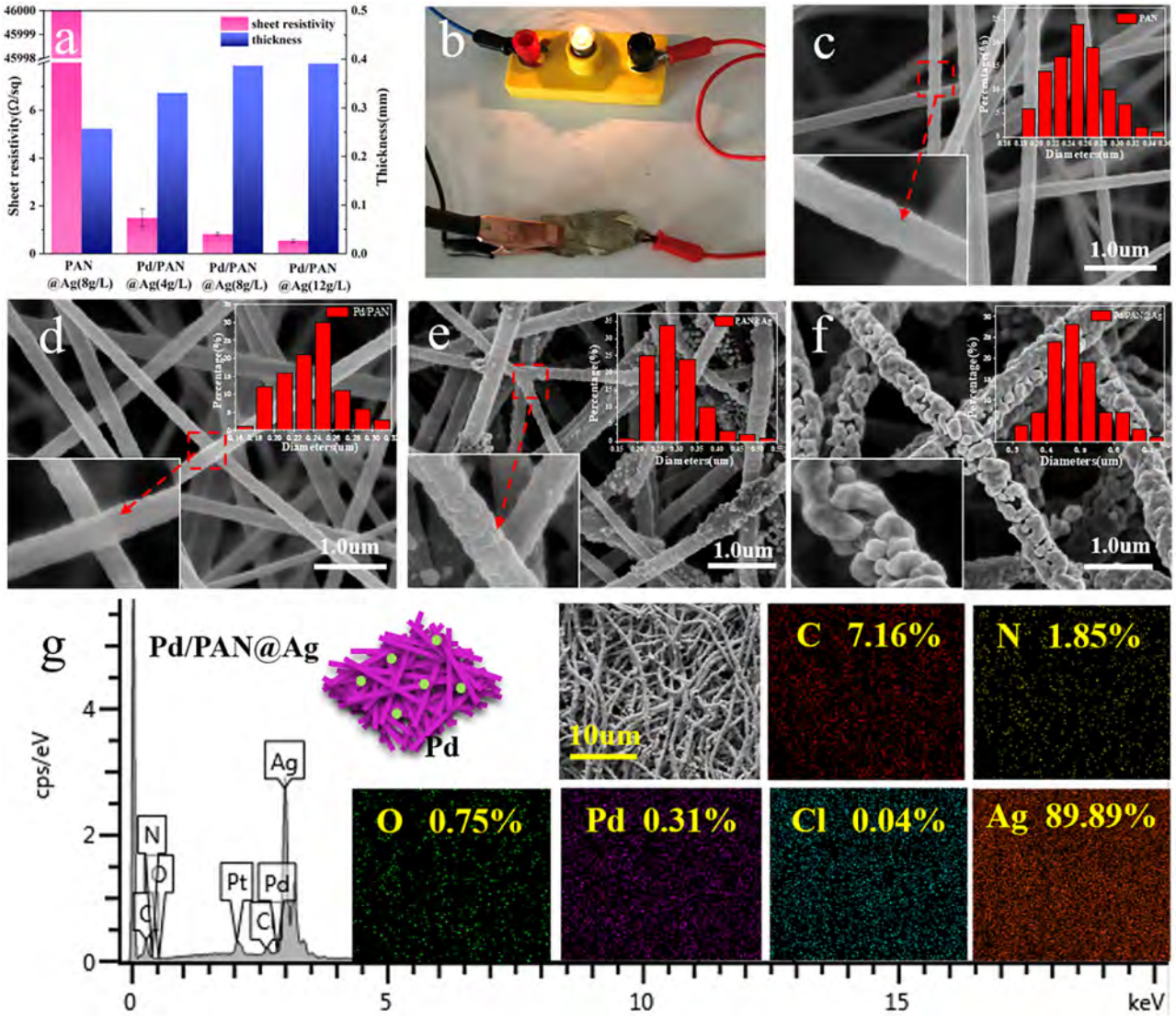

Fig. 2. Resistance variation, typical FESEM images and diameter distribution of the different samples: (a) electrical conductivity, (b) the circuit of a light bulb, (c) PAN, (d) Pd/PAN, (e) PAN @Ag and (f) Pd/PAN @Ag, (g) corresponding EDS mapping images of Pd/PAN@Ag nanofibrous membranes.

membrane in advance.

In order to analyze the thermal stability of the PAN and silver composite PAN, the TG curves are shown in Fig. 3(e). The weight loss after 550 °C can be attributed to inorganic materials in the composites [30]. For pure PAN, there are three noticeable weight loss steps, the first losses step at the mass is caused by a little side group and the continuous cyano group decomposition in oligomerization [32]. The loss process of the carbonation and broken cyclic structure lead to mass loss account for the second step occurring, the final step indicates the ulterior oxidation of the char based on the previous two steps [33]. The initial thermal degradation temperature of membranes after silver-plated is closely to that of PAN membrane [34]. The weight loss stages of silver-coated treated nanofibers are multiple platforms, which delays the initial and maximum decomposition temperatures compared with other samples and the heat stability of prepared membrane [21]. Therefore, the heat stability is basically unchanged by treatment, and the different final remaining weights illustrated that the remaining ingredient of metal silver is about 27.8%, which conforms to the weight gain rate of the material.

By x-ray diffraction, the characteristic diffraction patterns are analyzed to confirm the crystalline structure of Ag on the PAN nanofibrous membrane. In Fig. 3(g-i), the characteristic peaks are observed at 2θ values of 38.1°, 44.3°, 64.5°, 77.4°, and 81.3°, corresponding to the (1 1 1), (2 0 0), (2 2 0), (3 1 1) and (2 2 2) crystal faces of metallic silver [35]. Besides, there are no other prominent diffraction peaks, indicating that there is no impure crystal in the surface, and the face-centered cubic of silver on the sample [36] is successfully prepared. At the same time, we compare the peaks of different 2θ values. It can be seen that the peak height of 111 is 2.5 times higher than that of 200, indicating that silver has higher surface energy on the 111 sides and which leads to faster growth. By putting into the Scherrer formula to calculate, the average crystallite size of nano-silver on the nanofibrous membrane is around 159.50 nm.

3.3. Pressure sensing performance

Generally, sensitivity, response time and durability are the three fundamental and important indicators for evaluating the performance of pressure sensors. Sensitivity can be defined as the following formula: $S = \delta(\Delta C/C_0)/\delta P$, where ΔC is the varying capacitance, C_0 is the initial capacitance value (~47.76 pF) in large sensors and around 26.74 pf in the small size, and P is the applied pressure. The working range is confirmed when the pressure further increases to a certain value and the capacitance changes negligibly (< 0.01 pF) [37]. Fig. 4(a) presents

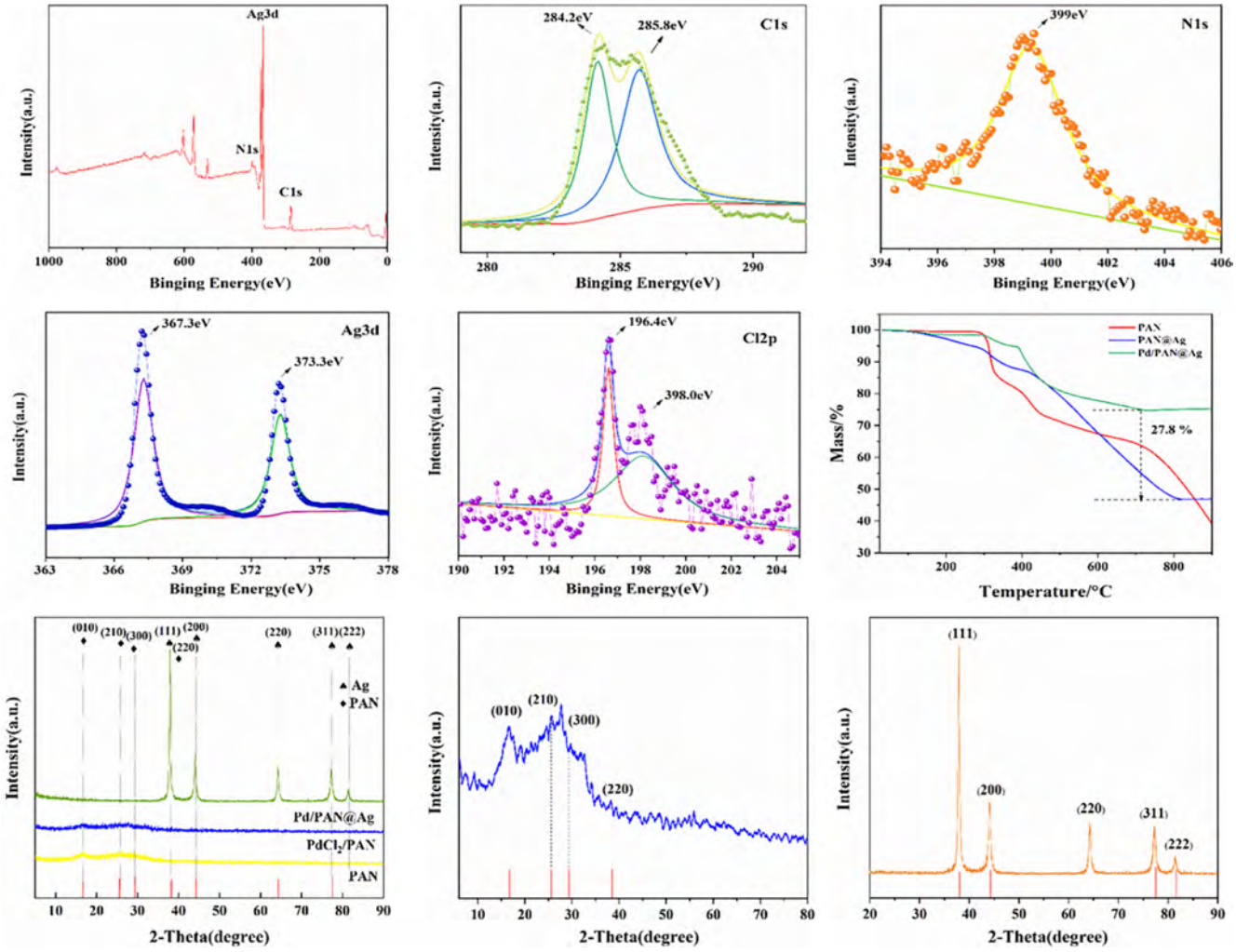

Fig. 3. XPS spectrum and core-level spectra, TG curves and XRD patterns. (a) XPS patterns of Pd/PAN@Ag, (b) XPS patterns of C1s, (c) XPS patterns of N1s, (d) XPS patterns of Ag3ds, (e) XPS patterns of Cl2p, (f) TG curves of three samples, (g) XRD patterns of three samples, (h) partially amplified XRD patterns of PAN, and (i) partially amplified XRD patterns of Pd/PAN @Ag.

the SEM image of the nylon layer, the morphology of the nylon netting with 400 mesh is presented, indicating exceedingly regular and orderliness staggered grid at the size of 400 um^2, which constructed a dielectric layer with a uniform distribution of micron-sized pores.

The testing and calculating results are presented in Fig. 4(b), the sensitivity of the high conductivity one is 1.49 kPa^{-1} in a range of low pressure (0–1 kPa, R^2 = 0.995), and 0.13 kPa^{-1} in high-pressure range (1–10 kPa, R^2 = 0.992). The declining sensitivity of another low conductivity is 1.14 kPa^{-1} (R^2 = 0.995) under the high working range 0–1 kPa and 0.12 kPa^{-1} (R^2 = 0.996) under 10 kPa. The change of capacitance is not obvious in the insulation area, according to the formula of $C = \varepsilon_0\varepsilon_r A/d$, when the electrode area contacting with the dielectric layer A is reduced, which results in low sensitivity. As the pressure further increases from 1 to 10 kPa, the similar sensitivity is ascribed to the slight change of the relative area. In sum, the above results indicate that the pressure sensor based on the high-conductivity nanofibrous electrode has higher sensitivity, and more inconspicuous response under large pressure range, implying this kind of sensor can be used for the detection of subtle movements.

The response speed is another critical performance of the strain sensor. An applying and removing cycle under approximately 0.2 kPa static pressure shown in Fig. 4(c). The fast response time is about 48 ms, which approach to the speed of human skin reaction (30–50 ms), and recovery time is captured around 68 ms. At each time point of transformational surface pressure, the capacitance value always undergoes a special mutation, uneven force may induce the edge effects, reducing the size of the sensor can alleviate this situation, so we use a small size sensor (15 × 15 mm^2) to adapt the small weight. Herein, our work will be compared with recently reported wearable capacitive pressure sensors [24,38–44]. In Fig. 4(d), The as-prepared sensor exhibits a high sensitivity of 1.49 kPa^{-1} and fast response time of 48 ms, it is comparable to the capacitive pressure sensors featured with fast response time, and the high sensitivity is superior to these fiber-based capacitive pressure sensors (circular points), and also surpass some elastic capacitive pressure sensors (triangle points) with microstructures maintaining a relatively thin thickness (0.57 mm). Moreover, compared with graphene/porous nylon networks, the use of the Pd/PAN@Ag electrode possesses more than four times of sensitivity, providing a new insight to assemble more sensors with excellent performance.

In order to measure the reproducible behavior of the strain sensor, incremental pressure between 1 and 10 kPa is applied, a typical loading and unloading curve exhibits a max hysteresis error around 7.55% under 0.2 kPa, as shown in Fig. 4(e). This recoverability attributes to the flexibility of sensor components and the peculiarity of the PI substrate. Different from the most elastomer with obvious viscoelasticity and hysteresis, the flat and thin PI tape is reproducible and improve the mechanical stability [6,45]. In order to further test the durability of the sensor, we applied pressure of 0.4 kPa on the equipment, and then performed 1000 loading/unloading cycles during 800 s to measure the performance (Fig. 4f). It is observed that after a large number of cycles,

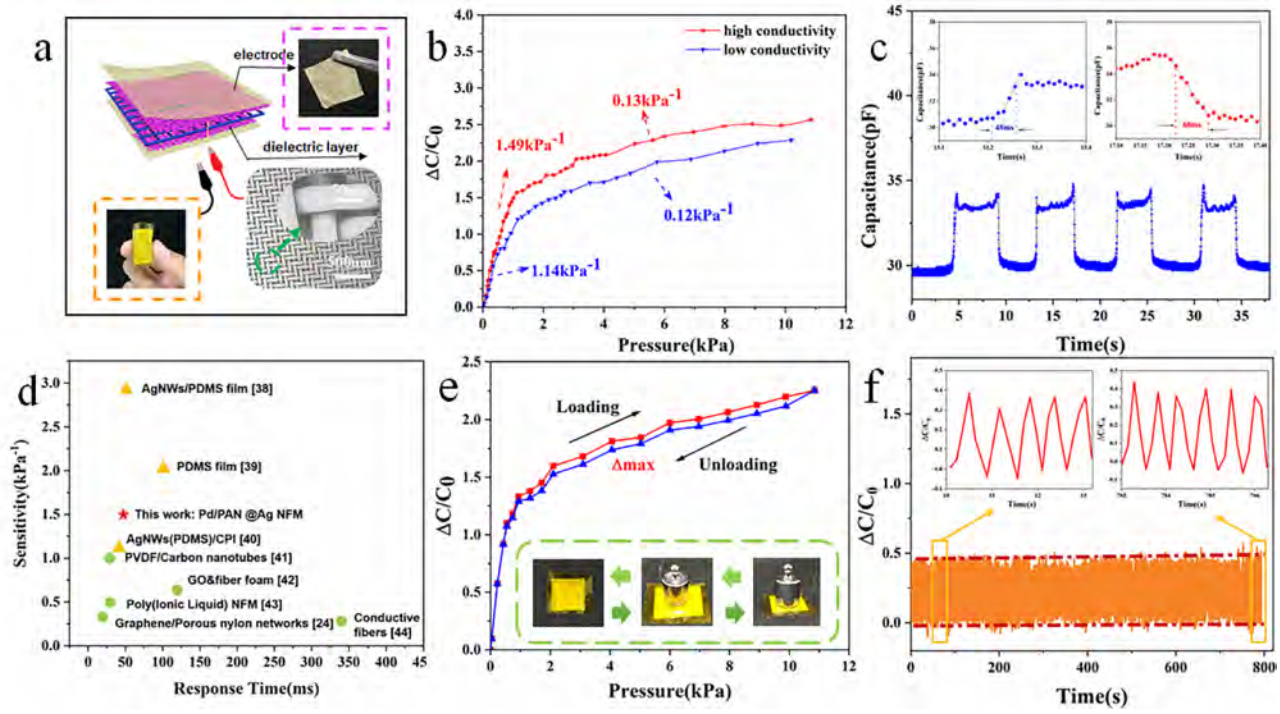

Fig. 4. Evaluation of the sensitivity of the capacitive pressure sensor. (a) The schematic diagram of the dielectric layer and the electrode layer. (b) Capacitance variation ($\Delta C/C_0$) – pressure relationship curve of the capacitive pressure sensor. (c) Capacitance changes under typical loading and unloading curve, (d) Comparison of recently reported fiber-based or elastic capacitive pressure sensors. (e) Response time of pressure sensor upon repeated pressure applying and removing cycle under 0.2 kPa. (f) Durability measure under a pressure of 0.4 kPa for more than 1000 times.

the sensor reflects a stable sensitivity, and has a high recognition for pressure to meet the expectation of future performance in a certain extent.

3.4. Applications in human motion detection

In order to further explore applications in dynamic response and human motion recognition, sensors of different sizes are placed on various surfaces with an adhesive tape, which is expected to check the practical performance of the human joints and corresponding items [10], and the original capacitance may change in different certain adhesion forces, but it shows the similar trend. First, the gloved finger applies different types of external force, such as pressing, twisting and stretching as shown in Fig. 5(a-c). The strain sensor is touched by a finger repeatedly for several times, the tactile sensors deform each time and the capacitance of real-time data is gathered. The output capacitance signal records three different curves, which explains that it can identify different types of stress visibly and has a good sensitivity and synchronization for distinguishing finger movements [43]. In order to further test the durability of finger pressure, the sensing device is pressured by finger under certain frequency and force (Fig. 5d). No significant signal degradation exhibits good stability and reproducibility in the test of 1000 press-release cycles.

Next, for the purpose of simulating the daily movement mode and observing the regularity of the change in capacitance value, sensors are fixed to the typical joints of wrists, knees, and elbows. The process of wrists bends at 60° and recovers to a group of consistent signals (Fig. 5e). Fig. 5(f) clearly illuminates two representative moments that the leg is lifted and declined, corresponding to the flexion and extension of the keen joint, the transition from the stretched state to the contracted state exhibits symmetrical waveform characteristics. As shown in Fig. 5(g), compared with the knee and wrist, the contact surface is relatively flat, its deformation is mainly caused by the expansion and bending, but for the elbow, because of the irregular muscle deformation, the electronic signal is more complicated [40]. Hence, the receiving waveforms have a little difference each time. These phenomena indicate a feasible skin-mountable property.

In addition, in view of high sensitivity in low pressure and low detection limit, we mount the sensor onto the mouse and facial muscles to monitor other physical and subtle physiological signals. Combing the shorter response time and recognizable finger movement, it can be extended to apply in mouses as shown in Fig. 5(h). We simulate the daily habits of mouse users, one click and double click at diverse speeds can be discerned, even it can distinguish by consecutive clicks during several hundred milliseconds [46]. When putting on the cheek as shown in Fig. 5(i), it can read out a smile or laugh as a strain sensor. The fluctuation of the curve is due to the vibration of the facial muscle action.

3.5. Simulation of ANSYS Workbench and principle analysis of the pressure sensor

To elucidate the sensing mechanism of the surface microstructure on the device, the finite element analysis models of ANSYS is applied to simulate the deformation process of the devices under applied pressure. Due to the symmetry condition of the structure, half of the model is considered. The diameter of nanofibers and the size of nano-silver on the surface are based on FESEM and XRD. The pore size and spacing of nylon mesh are based on SEM. Referred to relevant research [47–49], the Young's modulus, Poisson's ratio and density of samples are set (PAN: 19.6 MPa, 0.33, 1.18 g/cm^3; Nylon: 2.95 GPa, 0.398, 1.13 g/cm^3).

In order to simplify the simulation model, the microstructure of the Pd/PAN@Ag membranes and nylon netting are partitioned on each other, a 3 × 3 mesh array is simulated for force analysis in Fig. 6(a-f). First, the deformation of the membranes is concentrated in the pores of the nylon mesh (Fig. 6b-c). When the nanofibers are subjected to pressure, the nanofibers on the nylon fibers squeeze each other, and other nanofibers sink into the pores to accommodate the pressure at the pores. Second, the bending deformation is relatively uneven and

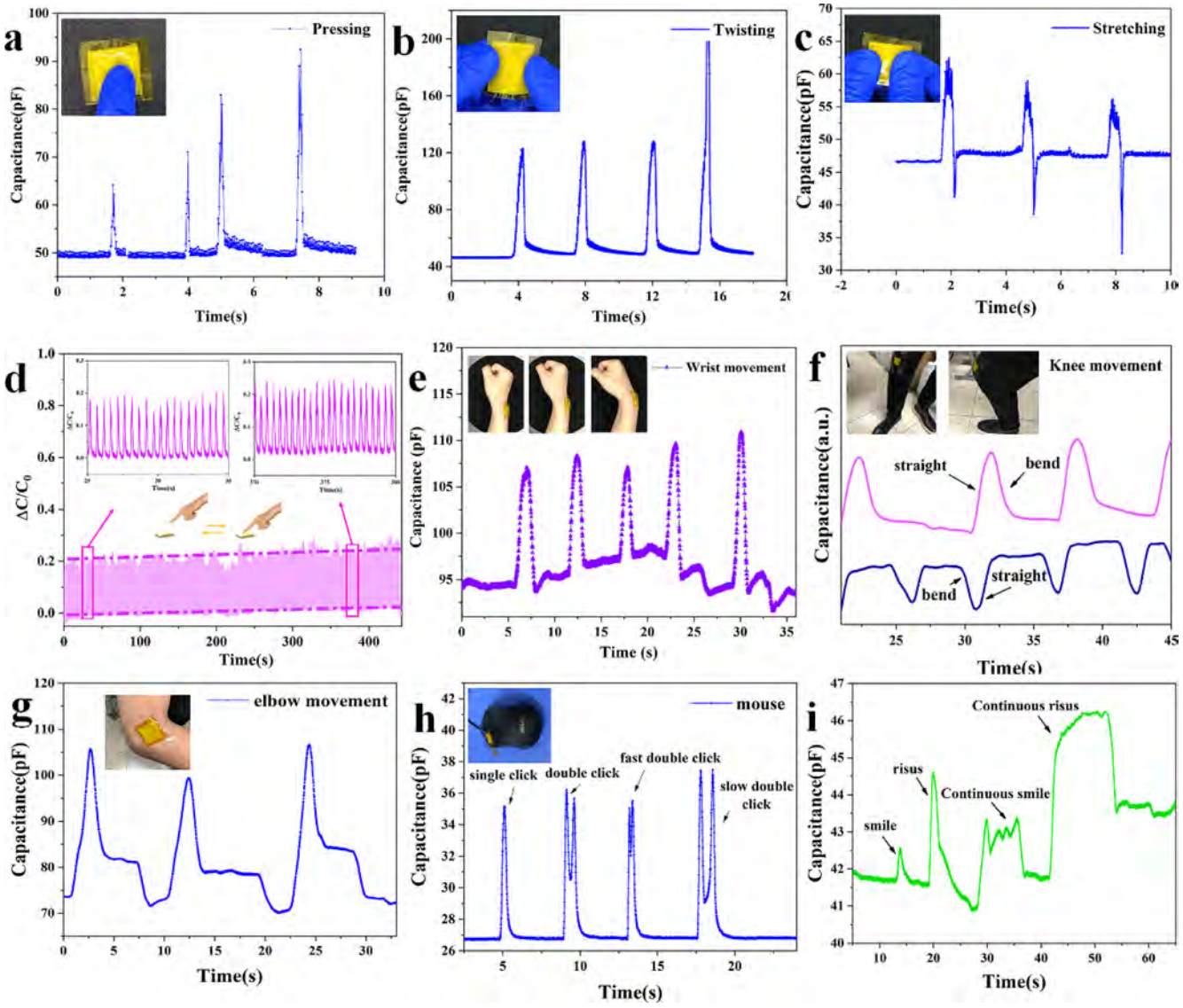

Fig. 5. The applications of the wearable capacitive sensor in human motion detection, the capacitance variation in response to finger movement and joint movement: (a) pressing, (b) twisting, and (c) stretching, (d) long-term stability of the pressure sensor during 1000 repetitive loading-unloading cycles by finger. (e) wrist movement, (f) knee movement, and (g) elbow movement. The applications of the wearable capacitive pressure sensors in physical and subtle physiological signals: (h) Different click on mouse keys. (i) The recorded facial muscle action.

focuses on the center of the hole as shown in Fig. 6(e-f), leading to present the specific capacitive signals. As expected, this result demonstrates the effects of the different finger and joint movements, and the simulation of the proposed model is in good accordance with the performance test. In summary, the intermediate layer is composed of a dielectric material (ε_{PA6} = 3.4) and air (ε_{air} = 1), according to the formula $\varepsilon = \varepsilon_a f + \varepsilon_b(1\text{-}f)$, where f is the volume ratio of different media. When the nanofibrous membrane is trapped in the pore, the air is extruded, and the dielectric substance ε replaces part of the air ε. Combining the changes of relative inter-planar spacing and area in the nylon layer, the function mechanism is explained by the formula of $\Delta C = (\varepsilon + \Delta\varepsilon)(A_0 + \Delta A)/(d_0\text{-}\Delta d)\text{-}C_0$.

As a qualitative illustration, electrospun nanofibers are interlaced distribution based on the reported square lattice as the structural characteristics [16]. The two models of nanofibers are set as the same thickness-to-length ratio (1:13), and the nano-silver of surface is simplified as the sphere and random distribution, a 2 × 3 vertical array is simulated for discussion. As demonstrated in Fig. 6(g-l), when the device is subjected to pressure, the change of the contact nodes is mainly contributed by a large number of nanofibers touching with the nylon layer. As a result, the relative area A as well as d increases significantly, consequently generating remarkable capacitance signals. Meanwhile, the contact area of the smooth nanofibers with uniform cross sections is much less than that of the protruding coral-like nanofibers with non-uniform cross sections, and the sensitivity of semicylinder microstructure is superior to the pyramid and semisphere microstructures [50]. This phenomenon is an important reason for high sensitivity.

4. Conclusions

In this study, we develop a microporous pressure sensor based on conductive nanofibrous membranes and high mesh nylon netting dielectric layers. Instead of the traditional electroless plating process, a small amount of activator is mixed into an electrospinning solution in advance, and then electroless silver plating on this membrane. This capacitive pressure sensor has high sensitivity of 1.49 kPa^{-1} (< 1 kPa) and 0.13 kPa^{-1} (1–10 kPa) with a low hysteresis of 7.55%. It also shows fast response (48 ms), relaxation time (68 ms) and durable stability under 1000 times repeated cycles. Benefiting from these properties, the sensor can monitor the movement of fingers and joints, and has

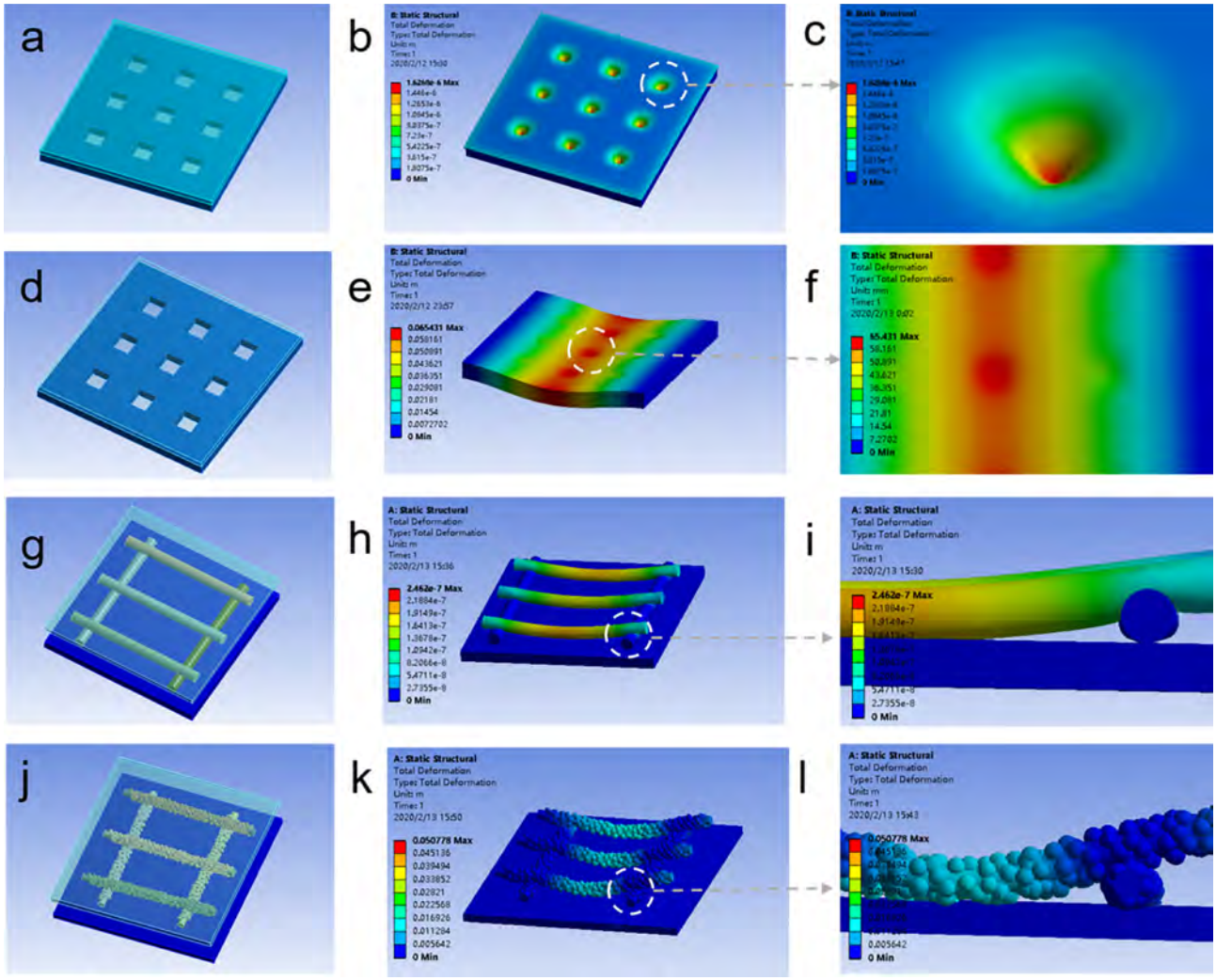

Fig. 6. The finite element analysis models of ANSYS are simulated and analyzed in the structural unit effects of pressure sensor models. (a) and (d) are mesh model based on nylon netting microstructure of sensor unit. (b) shows the deformation diagram of the nanofibrous membranes under certain pressure. (e) is the bending deformation diagram. (g) is the smooth nanofibers. (j) is the nanofibers based on the silver-plated coral-like surface. (h) and (k) show the deformation diagram of the nanofibers. (c), (f), (i) and (l) are their enlarged pictures, respectively.

potential applications in the mouse keys and facial muscles. The simulation of ANSYS is also used to explain the principle analysis of the high-sensitivity pressure sensor. In summary, this study provides an effective method of designing a functional pressure sensor with outstanding properties.

Declaration of Competing Interest

The authors declare that they have no known competing financial interests or personal relationships that could have appeared to influence the work reported in this paper.

Acknowledgement

This work was supported by National Science Foundation of China (NSFC) (No. 51403032).

References

[1] Y. Zang, F. Zhang, C.-A. Di, D. Zhu, Advances of flexible pressure sensors toward artificial intelligence and health care applications, Mater. Horiz. 2 (2015) 140–156.
[2] S.I. Rich, R.J. Wood, C. Majidi, Untethered soft robotics, Nat. Electron. 1 (2018) 102–112.
[3] S. Yao, A. Myers, A. Malhotra, F. Lin, A. Bozkurt, J.F. Muth, Y. Zhu, A wearable hydration sensor with conformal nanowire electrodes, Adv. Healthc. Mater. 6 (2017) 1601159.
[4] Z. Wang, W. Wang, D. Yu, Pressure responsive PET fabrics via constructing conductive wrinkles at room temperature, Chem. Eng. J. 330 (2017) 146–156.
[5] S. Wan, H. Bi, Y. Zhou, X. Xie, S. Su, K. Yin, L. Sun, Graphene oxide as high-performance dielectric materials for capacitive pressure sensors, Carbon 114 (2017) 209–216.
[6] B. You, C.J. Han, Y. Kim, B.-K. Ju, J.-W. Kim, A wearable piezocapacitive pressure sensor with a single layer of silver nanowire-based elastomeric composite electrodes, J. Mater. Chem. A 4 (2016) 10435–10443.
[7] Y. Joo, J. Yoon, J. Ha, T. Kim, S. Lee, B. Lee, C. Pang, Y. Hong, Highly sensitive and bendable capacitive pressure sensor and its application to 1 V operation pressure-sensitive transistor, Adv. Electron. Mater. 3 (2017) 1600455.
[8] W. Gao, S. Emaminejad, H.Y.Y. Nyein, S. Challa, K. Chen, A. Peck, H.M. Fahad, H. Ota, H. Shiraki, D. Kiriya, D.H. Lien, G.A. Brooks, R.W. Davis, A. Javey, Fully integrated wearable sensor arrays for multiplexed in situ perspiration analysis, Nature 529 (2016) 509–514.
[9] N. Shao, J. Wu, X. Yang, J. Yao, Y. Shi, Z. Zhou, Flexible capacitive pressure sensor based on multi-walled carbon nanotube electrodes, Micro. Nano Lett. 12 (2017) 45–48.
[10] J. Qiu, X. Guo, R. Chu, S. Wang, W. Zeng, L. Qu, Y. Zhao, F. Yan, G. Xing, Rapid-response, low detection limit, and high-sensitivity capacitive flexible tactile sensor based on three-dimensional porous dielectric layer for wearable electronic skin, ACS Appl. Mater. Interfaces 11 (2019) 40716–40725.
[11] S. Luo, J. Yang, X. Song, X. Zhou, L. Yu, T. Sun, C. Yu, D. Huang, C. Du, D. Wei, Tunable-sensitivity flexible pressure sensor based on graphene transparent electrode, Solid-State Electron. 145 (2018) 29–33.
[12] H. Kim, G. Kim, T. Kim, S. Lee, D. Kang, M.S. Hwang, Y. Chae, S. Kang, H. Lee, H.G. Park, W. Shim, Transparent, flexible, conformal capacitive pressure sensors with nanoparticles, Small 14 (2018) 1703432.

[13] O. Atalay, A. Atalay, J. Gafford, C. Walsh, A highly sensitive capacitive-based soft pressure sensor based on a conductive fabric and a microporous dielectric layer, Adv. Mater. Technol. 3 (2018) 1700237.
[14] Z. Qiu, Y. Wan, W. Zhou, J. Yang, J. Yang, J. Huang, J. Zhang, Q. Liu, S. Huang, N. Bai, Z. Wu, W. Hong, H. Wang, C.F. Guo, Ionic skin with biomimetic dielectric layer templated from calathea zebrine leaf, Adv. Funct. Mater. 28 (2018) 1802343.
[15] W. Cheng, J. Wang, Z. Ma, K. Yan, Y. Wang, H. Wang, S. Li, Y. Li, L. Pan, Y. Shi, Flexible pressure sensor with high sensitivity and low hysteresis based on a hierarchically microstructured electrode, IEEE Electron Device Lett. 39 (2018) 288–291.
[16] S. Lee, A. Reuveny, J. Reeder, S. Lee, H. Jin, Q. Liu, T. Yokota, T. Sekitani, T. Isoyama, Y. Abe, Z. Suo, T. Someya, A transparent bending-insensitive pressure sensor, Nat. Nanotechnol. 11 (2016) 472–478.
[17] T. Wang, Y. Zhang, Q. Liu, W. Cheng, X. Wang, L. Pan, B. Xu, H. Xu, A. Self-Healable, Highly stretchable, and solution processable conductive polymer composite for ultrasensitive strain and pressure sensing, Adv. Funct. Mater. 28 (2018) 1705551.
[18] Z. Wang, W. Wang, Z. Jiang, D. Yu, Low temperature sintering nano-silver conductive ink printed on cotton fabric as printed electronics, Prog. Org. Coat. 101 (2016) 604–611.
[19] Z. Wang, W. Wang, Z. Jiang, D. Yu, A novel and simple method of printing flexible conductive circuits on PET fabrics, Appl. Surf. Sci. 396 (2017) 208–213.
[20] W. Wang, W. Li, C. Gao, W. Tian, B. Sun, D. Yu, A novel preparation of silver-plated polyacrylonitrile fibers functionalized with antibacterial and electromagnetic shielding properties, Appl. Surf. Sci. 342 (2015) 120–126.
[21] X. Zhong, R. Li, Z. Wang, W. Wang, D. Yu, Titanium dioxide/quaternary phosphonium salts/polyacrylonitrile composite nanofibrous membranes with high antibacterial properties and ultraviolet resistance efficiency, J. Mater. Sci. 54 (2019) 13322–13333.
[22] L. Shen, L. Yu, M. Wang, X. Wang, M. Zhu, B.S. Hsiao, Green fabrication of Ag coated polyacrylonitrile nanofibrous composite membrane with high catalytic efficiency, J. Nanosci. Nanotechnol. 15 (2015) 5004–5012.
[23] L. Zhang, X. Gong, Y. Bao, Y. Zhao, M. Xi, C. Jiang, H. Fong, Electrospun nanofibrous membranes surface-decorated with silver nanoparticles as flexible and active/sensitive substrates for surface-enhanced Raman scattering, Langmuir 28 (2012) 14433–14440.
[24] Z. He, W. Chen, B. Liang, C. Liu, L. Yang, D. Lu, Z. Mo, H. Zhu, Z. Tang, X. Gui, Capacitive pressure sensor with high sensitivity and fast response to dynamic interaction based on graphene and porous nylon networks, ACS Appl. Mater. Interfaces 10 (2018) 12816–12823.
[25] P. Cataldi, S. Dussoni, L. Ceseracciu, M. Maggiali, L. Natale, G. Metta, A. Athanassiou, I.S. Bayer, Carbon nanofiber versus graphene-based stretchable capacitive touch sensors for artificial electronic skin, Adv. Sci. (Weinh.) 5 (2018) 1700587.
[26] T. Luangpipat, I.R. Beattie, Y. Chisti, R.G. Haverkamp, Gold nanoparticles produced in a microalga, J. Nanopart. Res. 13 (2011) 6439–6445.
[27] J. Bai, Y. Li, S. Yang, J. Du, S. Wang, C. Zhang, Q. Yang, X. Chen, Synthesis of AgCl/PAN composite nanofibres using an electrospinning method, Nanotechnology 18 (2007) 305601.
[28] V. Vaiano, M. Matarangolo, J.J. Murcia, H. Rojas, J.A. Navío, M.C. Hidalgo, Enhanced photocatalytic removal of phenol from aqueous solutions using ZnO modified with Ag, Appl. Catal., B 225 (2018) 197–206.
[29] J. Liu, W.X. He, X.J. Wei, A.Q. Diao, J.M. Xie, X.M. Lü, Ag-embedded MnO nanorod: facile synthesis and oxygen reduction, CrystEngComm 17 (2015) 7646–7652.
[30] W. Wang, W. Li, J. Ye, R. Zhang, J. Wang, The preparation and characterization of the cross-linked Ag–AgCl/polypyrrole nanocomposite, Synth. Met. 160 (2010) 2203–2207.
[31] A.S. Romanchenko, Y.L. Mikhlin, An XPS study of products formed on pyrite and pyrrhotine by reacting with palladium(II) chloride solutions, J. Struct. Chem. 56 (2015) 531–537.
[32] P. Joseph, S. Tretsiakova-McNally, Combustion behaviours of chemically modified polyacrylonitrile polymers containing phosphorylamino groups, Polym. Degrad. Stab. 97 (2012) 2531–2535.
[33] Y. Ren, T. Tian, L. Jiang, Y. Guo, Fabrication of chitosan-based intumescent flame retardant coating for improving flame retardancy of polyacrylonitrile fabric, Molecules 24 (2019) 3749.
[34] D. Yu, G. Kang, W. Tian, L. Lin, W. Wang, Preparation of conductive silk fabric with antibacterial properties by electroless silver plating, Appl. Surf. Sci. 357 (2015) 1157–1162.
[35] Y.-S. Park, C.Y. An, P.K. Kannan, N. Seo, K. Zhuo, T.K. Yoo, C.-H. Chung, Fabrication of dendritic silver-coated copper powders by galvanic displacement reaction and their thermal stability against oxidation, Appl. Surf. Sci. 389 (2016) 865–873.
[36] C. Wang, W. Wang, L. Zhang, S. Zhong, D. Yu, Electrospinning of PAN/Ag NPs nanofiber membrane with antibacterial properties, J. Mater. Res. 34 (2019) 1669–1677.
[37] X. Zeng, Z. Wang, H. Zhang, W. Yang, L. Xiang, Z. Zhao, L.M. Peng, Y. Hu, Tunable, ultrasensitive, and flexible pressure sensors based on wrinkled microstructures for electronic skins, ACS Appl. Mater. Interfaces 11 (2019) 21218–21226.
[38] X. Shuai, P. Zhu, W. Zeng, Y. Hu, X. Liang, Y. Zhang, R. Sun, C.P. Wong, Highly sensitive flexible pressure sensor based on silver nanowires-embedded polydimethylsiloxane electrode with microarray structure, ACS Appl. Mater. Interfaces 9 (2017) 26314–26324.
[39] L. Ma, X. Shuai, Y. Hu, X. Liang, P. Zhu, R. Sun, C.-P. Wong, A highly sensitive and flexible capacitive pressure sensor based on a micro-arrayed polydimethylsiloxane dielectric layer, J. Mater. Chem. C 6 (2018) 13232–13240.
[40] Y. Wan, Z. Qiu, Y. Hong, Y. Wang, J. Zhang, Q. Liu, Z. Wu, C.F. Guo, A highly sensitive flexible capacitive tactile sensor with sparse and high-aspect-ratio microstructures, Adv. Electron. Mater. 4 (2018) 1700586.
[41] X. Yang, Y. Wang, X. Qing, A flexible capacitive sensor based on the electrospun PVDF nanofiber membrane with carbon nanotubes, Sens. Actuators, A 299 (2019) 111579.
[42] Y.Q. Liu, Y.L. Zhang, Z.Z. Jiao, D.D. Han, H.B. Sun, Directly drawing high-performance capacitive sensors on copying tissues, Nanoscale 10 (2018) 17002–17006.
[43] Z. Wang, Y. Si, C. Zhao, D. Yu, W. Wang, G. Sun, Flexible and washable poly(ionic liquid) nanofibrous membrane with moisture proof pressure sensing for real-life wearable electronics, ACS Appl. Mater. Interfaces 11 (2019) 27200–27209.
[44] A. Chhetry, H. Yoon, J.Y. Park, A flexible and highly sensitive capacitive pressure sensor based on conductive fibers with a microporous dielectric for wearable electronics, J. Mater. Chem. C 5 (2017) 10068–10076.
[45] C.J. Han, B.-G. Park, M. Suk Oh, S.-B. Jung, J.-W. Kim, Photo-induced fabrication of Ag nanowire circuitry for invisible, ultrathin, conformable pressure sensors, J. Mater. Chem. C 5 (2017) 9986–9994.
[46] H. Kou, L. Zhang, Q. Tan, G. Liu, H. Dong, W. Zhang, J. Xiong, Wireless wide-range pressure sensor based on graphene/PDMS sponge for tactile monitoring, Sci. Rep. 9 (2019) 3916.
[47] S.-F. Li, J.-P. Chen, W.-T. Wu, Electrospun polyacrylonitrile nanofibrous membranes for lipase immobilization, J. Mol. Catal. B: Enzym. 47 (2007) 117–124.
[48] M. Miao, J. McDonnell, L. Vuckovic, S.C. Hawkins, Poisson's ratio and porosity of carbon nanotube dry-spun yarns, Carbon 48 (2010) 2802–2811.
[49] E. Ozen, A. Kiziltas, E.E. Kiziltas, D.J. Gardner, Natural fiber blend-nylon 6 composites, Polym. Composite. 34 (2013) 544–553.
[50] S. Peng, P. Blanloeuil, S. Wu, C.H. Wang, Rational design of ultrasensitive pressure sensors by tailoring microscopic features, Adv. Mater. Interfaces 5 (2018) 1800403.